Supplementary Material Figure legends

Figure S1. The pLL is truncated in *krm1*^{nl10} adults

(**A,B**) DASPEI labeling of 4 months post fertilization (mpf) *Tg(cldnB:GFP)* expressing wild-type and *krm1*^{nl10} mutant adults. (**A**) A wild-type adult (24 mm in length) with DAPSEI labeled NMs on the trunk (blue arrows) and tail (blue brackets). (**B**) A 21 mm *krm1*^{nl10} mutant adult lacks the posterior-most trunk NMs (blue arrows) and all tail NMs.

Figure S2. The *krm1*^{nl10} mutation results in multiple cDNA splice variants

(**A**) Genomic DNA sequence for *kremen1* from wild-type and *krm1*^{nl10} mutant embryos showing the single base pair mutation from thymine (T) to cytosine (C; red asterisk) in the exon 6 splice donor site (black bar). (**B**) Schematic showing exons of wild-type *krm1*; the *krm1*^{nl10} lesion is located between exons 6 and 7 (red arrow). (**C**) Schematic representation of variant cDNAs generated from *krm1*^{nl10} embryos. (**D**) RT-PCR showing a single *krm1* cDNA band from wild-type embryos and multiple cDNA products from *krm1*^{nl10} embryos (see *krm1* primers in Materials and Methods). (**E**) Schematic showing wild-type Krm1 protein, including the signal peptide (SP), Kringle domain, WSC domain, CUB domain, Transmembrane domain and a short intracellular domain. Predicted protein variants from resulting from cryptic splicing of *krm1*^{nl10} . All schematics are not drawn to scale. (**F**) Quantification of *krm1* mRNA rescue following injection of

krm1 mRNA into embryos derived from *krm1*^{nl10}/+ X *krm1*^{nl10}/+ crosses. Injection of 200 pg/nl of *krm1* mRNA significantly increased the percentage of embryos that formed tc NMs (76% in uninjected and 98% in *krm1* mRNA injected), but did not affect NM number in wild-type embryos (n=51-58 embryos per condition; ***p*<0.001, *z*-test). In contrast injection of *krm1*^{nl10} V1 or V2 isoforms did not rescue NM number (74% in V1 injected and 76% in V2 injected embryos, n=36-49 embryos per condition).

Figure S3. Expression of *krm1, dkk1b* and *dkk2* partially overlaps throughout the embryo

(**A-B**) Expression domains of *krm1* and its ligands *dkk1b* and *dkk2* in 30 hpf wild-type embryos. (A) *krm1* is expressed in the mid-hindbrain boundary (mhb), lens (le), otic vesicle (ov), posterior lateral line primordium (pLLP) and the fin fold (ff). (**B**) *dkk1b* is expressed in the le, ov, pLLP and ff. (**C**) *dkk2* is expressed in the mhb, le, ov and pLLP.

Figure S4. The Wnt receptors *lrp5* and *lrp6* are expressed in the pLLP

(**A-B**) Expression of *lrp5* (**A**) and *lrp6* (**B**) throughout the primordia at 36 hpf in wild-type embryos. Scale bars=20 μm.

Figure S5. Cell death is increased in *krm1*^{nl10} mutant primordia

(A-B’’’) Confocal projections of 40 hpf wild-type (**A-A’’’**) and *krm1*^{nl10} (**B-B’’’**) labeled with activated Caspase3 antibody. Scale bars=20 µm. (n=35 embryos per condition, **p*<0.01, Fisher’s Exact Test).

Figure S6. Wnt activity is decreased following Krm1 knockdown.

(**A-D’’’**) Confocal projections of wild-type and *kremen1* morphant embryos expressing the Wnt sensor *Tg(7xtcf-siam:eGFP)* (green); nuclei are labeled with DAPI (blue). (**A-A’’, C-C’’**) GFP is expressed in cells of the leading part of a wild-type pLLP at 36 and 40 hpf. (**B-B’’,D-D’’**) In *kremen1*-MO injected embryos, GFP-positive cells are located throughout the pLLP, most are incorporated into proto-NMs (yellow arrows) and notably reduced in the leading region. By 40 hpf, the index of GFP-positive cells is significantly reduced in *kremen1* morphants (**E**). (**F**) The index of GFP in the leading zone of the pLLP (the caudal-most 30 cells of the pLLP) is significantly reduced in *kremen1* morphants at 36 and 40 hpf as compared to wild-type controls (n=10-12 embryos/condition; ***p*<0.001 Student’s *t*-test). Scale bars=20µm. (**G**) The mean fluorescence intensity of GFP-positive cells, measured in arbitrary units (A.U.), was significantly reduced in morphant primordia at both 36 and 40 hpf (n=10-12 embryos/condition; ***p*<0.001 Student’s *t*-test).

Figure S7. Members of the Fgf pathway are expressed in wild-type and *krm1*^{nl10} primordia

(**A-F**) Expression of *fgf10a* in wild-type and *krm1*^{nl10} primordia between 32 and 40 hpf. In wild-type embryos, *fgf10a* is expressed in the leading region of the primordia at 32, 36 and 40 hpf (**A,C,E**). A similar expression pattern for *fgf10a* was seen in *krm1*^{nl10} primordia (**B,D,F**). (**G-L**) Expression of the Fgf target *pea3* between 32 and 40 hpf. In wild-type (**G,I,K**) and *krm1*^{nl10} (**H,J,L**) embryos, expression of *pea3* is seen in the mid-zone of the primordia. Scale bars=20 µm.

Figure S8. Expression domains of chemokine receptors are not altered in *krm1*^{nl10} mutants

(**A-D**) Expression of *cxcr4b* and *cxcr7b* at 36 hpf in the primordia of wild-type and *krm1*^{nl10} mutants. *cxcr4b* is expressed in the leading and mid-zones of wild-type (**A**) and *krm1*^{nl10} (**B**) primordia. *cxcr7b* is expressed in the trailing zone of the wild-type (**C**) and mutant (**D**) primordia. Scale bars=20 µm.

Figure S9. pLL formation in mosaic embryos that contain *krm1*^{nl10}, *Tg(hsp701:dkk1b-GFP)* and *lef1*^{nl2} cells

(**A-E'**) Confocal projections of chimeric embryos with rhodamine-labeled donor cells (red) in *Tg(cldnB:GFP)*-positive hosts. At 24 hpf, donor cells are present in the leading region of primordia in wild-type to wild-type chimeras (**A**), wild-type to *krm1*^{nl10} (**B**), *krm1*^{nl10} to wild-type (**C**), *Tg(hsp701:dkk1b-GFP)* to wild-type (**D**) and wild-type to *lef1*^{nl2} mutants (**E**). At 2 dpf, pLL extension and terminal cluster (tc) formation was seen in wild-type to wild-type (**A'**), *krm1*^{nl10} to wild-type (**C'**)

and wild-type to *lef1*^{nl2} (**E'**). pLL formation was truncated in wild-type to *krm1*^{nl10} (**B'**) and *Tg(hsp701:dkk1b-GFP)* to wild-type (**D'**) chimeras. Scale bars=20 µm.

Figure S10. Cellular proliferation is not rescued by treatment with SU5402

(**A-D'**) Confocal projections of BrdU incorporation (red) in wild-type and *krm1*^{n10} embryos treated with DMSO or SU5402 between 24 and 34 hpf. BrdU label is present in the leading pLLP cells in DMSO treated wild-type (A-A'), but not mutant embryos (**C-C'**). SU5402 treatment resulted in reduced leading region BrdU incorporation in wild-type embryos (**B-B'**), but incorporation was not altered in SU5402 treated *krm1*^{nl10} mutants (**D-D'**). Scale bars=20 µm. (**E**) Quantification of the index of total BrdU incorporation in the pLLP showing no significant change in control versus treated wild-type embryos or control versus treated *krm1*^{nl10} mutants (n=11 embryos per condition, Student's *t*-test). (**E**) Quantification of the index of BrdU incorporation in the leading region of the pLLP shows a significant decrease in SU5402 treated wild-type embryos, but no change in *krm1*^{nl10} mutants (n=11 embryos per condition, Student's *t*-test).

Figure S11. Morpholino knockdown of Dkk1b and Dkk2 rescues NM number in *krm1*^{n10} mutants

(**A-C**) Injections of splice-blocking morpholinos against *dkk1b* (*dkk1b*-MO) and *dkk2* (*dkk2*-MO) result in improperly spliced RT-PCR products. (**A**) Schematic of the *dkk1b* gene, showing the location of RT-PCR primers (see Material and Methods; black arrows; 1b F/1b R). The *dkk1b*-MO blocks a splice donor site for

exon 1/intron 1. (**B**) Schematic of *dkk2* gene showing the location of RT-PCR primers (see Material and Methods; black arrows; 2 F/2 R). The *dkk2*-MO blocks the splice donor site for exon 2/intron 2. (**C**) RT-PCR using cDNA generated from uninjected or morphant embryos. Injection of *dkk1b*-MO or *dkk2*-MO results in misspliced transcripts. (**D**) Injections of *dkk1b*-MO, *dkk2*-MO or *dkk1b/2*-MOs did not alter the number of NMs deposited in wild-type embryos as compared to *p53*-MO injected controls. NM number was significantly increased in *krm1*^{nl10} mutants injected with *dkk1b*-MO, *dkk2*-MO or *dkk1b/2*-MOs as compared to *p53*-MO injected controls. (n=8 embryos per condition; $p>0.001$, one-way ANOVA). (**E**) NM spacing in wild-type embryo was not significantly altered by injection of *p53*-MO, nor were *krm1*^{nl10} mutants injected with *p53*-MO significantly different from uninjected controls NMs (n=10 embryos per condition, two-way ANOVA with replication).

Figure S12. Ectopic expression of Dkk1b-mTangerine results in decreased NM number and pLL truncation

(**A-D**) Confocal projections of 2 dpf embryos with ectopic expression Dkk1b-mTangerine (red) driven by heat-shock at 25 hpf. (**A**) Uninjected wild-type embryo show full pLL extension and terminal cluster (tc) formation, while uninjected *krm1*^{nl10} mutants show pLL truncation (**B**; yellow arrowhead). Dkk1b-mTangerine expression results in truncated pLL extension in both wild-type (**C**; yellow arrowhead) and *krm1*^{nl10} (**D**; yellow arrowhead) embryos. Scale bars=20 µm. (**E**) Quantification of NM number at 2 dpf; there is a significant decrease in

NM between uninjected control embryos (wild-type and *krm1*^{nl10} mutants) and embryos expressing Dkk1b-mTangerine (n=15, ***p*<0.001, two-way ANOVA with replication). There was no difference in NM number between wild-type and mutants expressing Dkk1b-mTangerine (n=15; Tukey's Post-Hoc Test).

Figure S13. Schematic model of Kremen1 activity in the pLLP

(**A**) In the wild-type pLLP, Kremen1 is expressed in the leading and mid-region of the pLLP. Dkk1b and Dkk2 are expressed in the mid-and trailing regions of the pLLP and are excluded from the leading region. Wnt signaling is active in the leading region and absent in the mid-and trailing regions, where Fgf signaling is active. (**B**) The *krm1*^{nl10} mutant pLLP lacks Kremen1 function, allowing for the spread of Dkk and inhibition of Wnt signaling in the leading region, resulting in truncated of pLL formation.

Figure S1

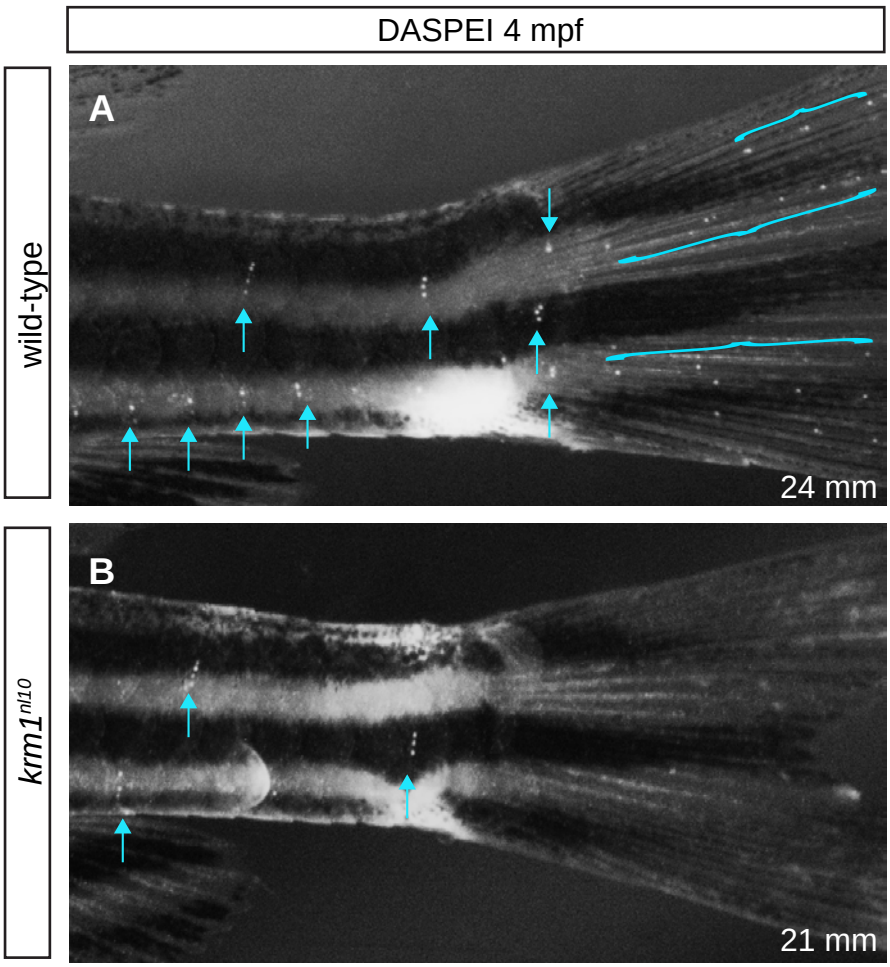

Figure S2

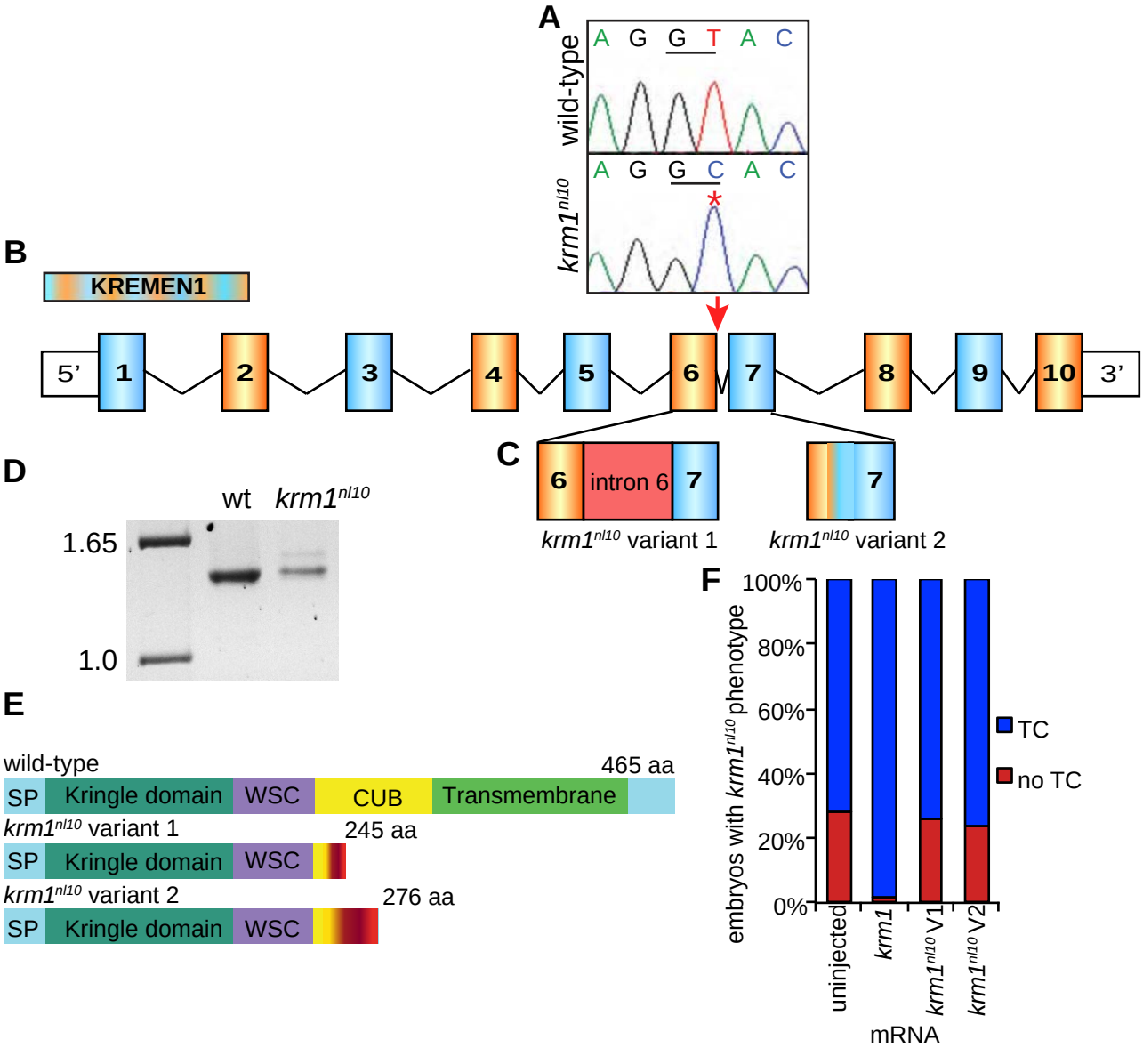
A
wild-type
A G G T A C
krm1nl10
A G G C A C
*
B
KREMEN1
5'
1
2
3
4
5
6
7
8
9
10
3'
C
6
intron 6
7
krm1nl10 variant 1
7
krm1nl10 variant 2
D
wt
krm1nl10
1.65
1.0
E
wild-type
465 aa
SP
Kringle domain
WSC
CUB
Transmembrane
krm1nl10 variant 1
245 aa
SP
Kringle domain
WSC
krm1nl10 variant 2
276 aa
SP
Kringle domain
WSC
F
embryos with krm1nl10 phenotype
100%
80%
60%
40%
20%
0%
TC
no TC
uninjected
krm1
krm1nl10V1
krm1nl10V2
mRNA

Figure S3

krm1

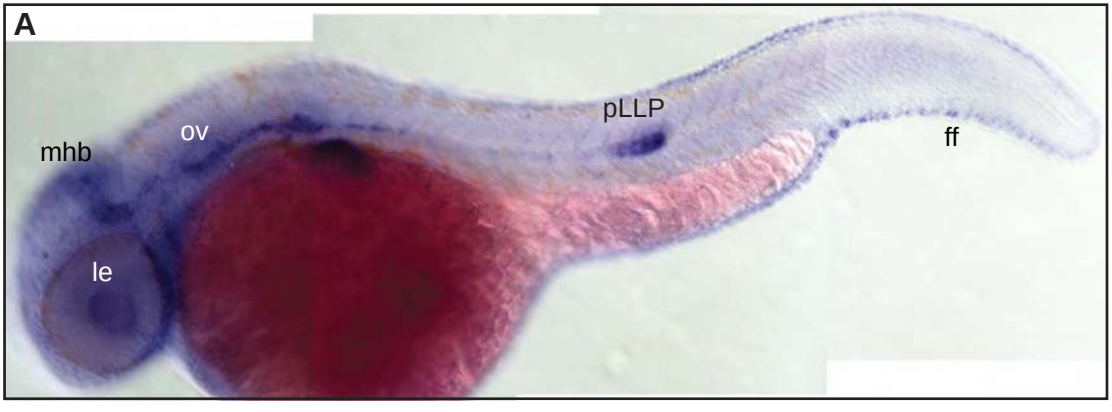

dkk1b

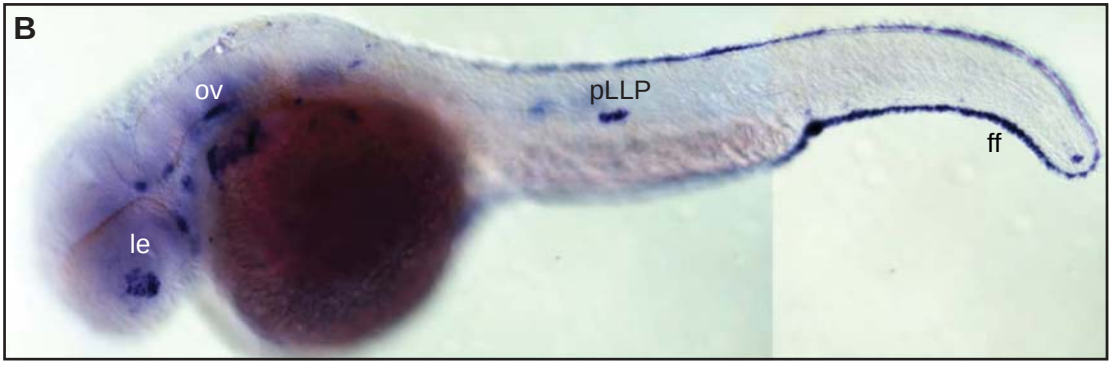

dkk2

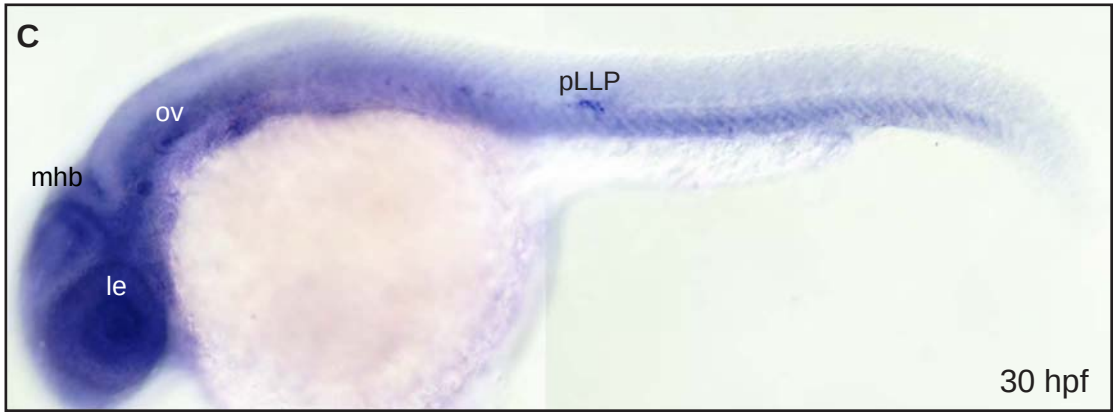

Figure S4

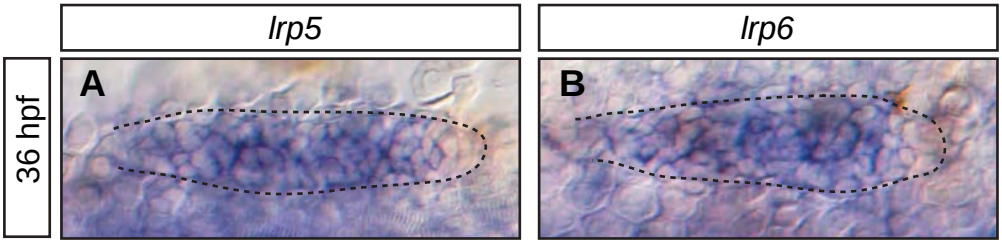

Figure S5

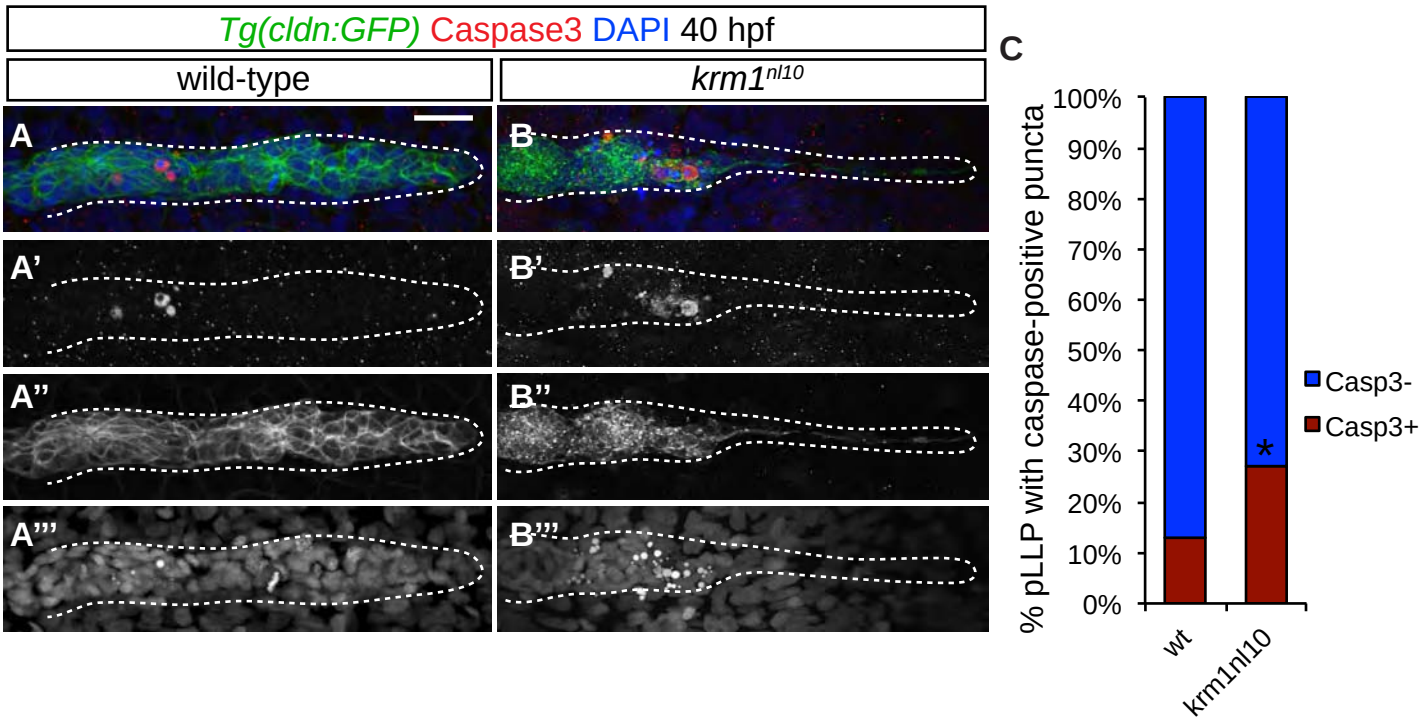
Tg(cldn:GFP) Caspase3 DAPI 40 hpf
wild-type
krm1nl10
A
B
A'
B'
A''
B''
A'''
B'''
C
% pLLP with caspase-positive puncta
100%
90%
80%
70%
60%
50%
40%
30%
20%
10%
0%
Casp3-
Casp3+
*
wt
krm1nl10

Figure S6

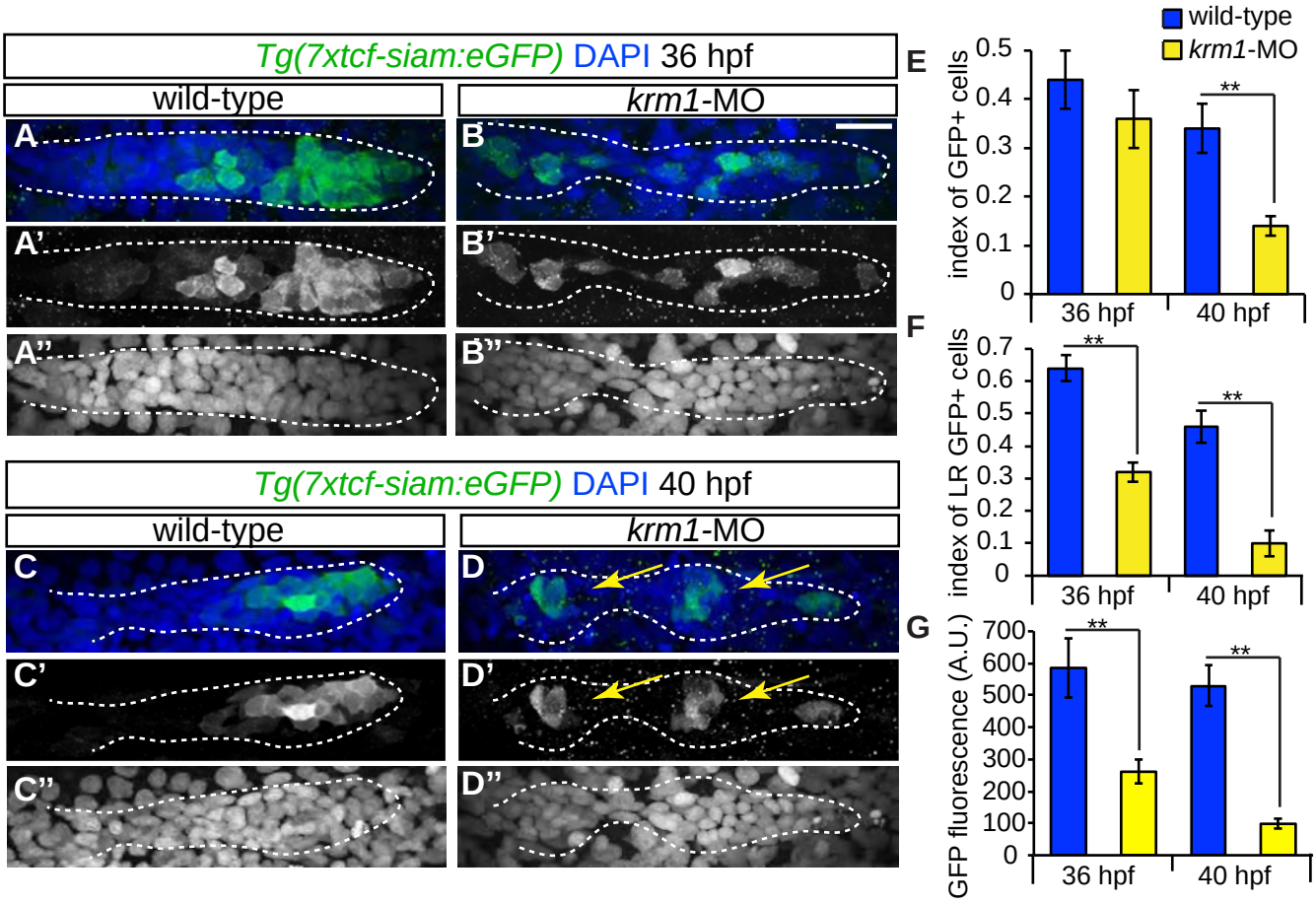
Tg(7xtcf-siam:eGFP) DAPI 36 hpf
wild-type
krm1-MO
A
A'
A''
B
B'
B''
Tg(7xtcf-siam:eGFP) DAPI 40 hpf
wild-type
krm1-MO
C
C'
C''
D
D'
D''
E
wild-type
krm1-MO
index of GFP+ cells
0.5
0.4
0.3
0.2
0.1
0
**
36 hpf
40 hpf
F
index of LR GFP+ cells
0.7
0.6
0.5
0.4
0.3
0.2
0.1
0
**
**
36 hpf
40 hpf
G
GFP fluorescence (A.U.)
700
600
500
400
300
200
100
0
**
**
36 hpf
40 hpf

Figure S7

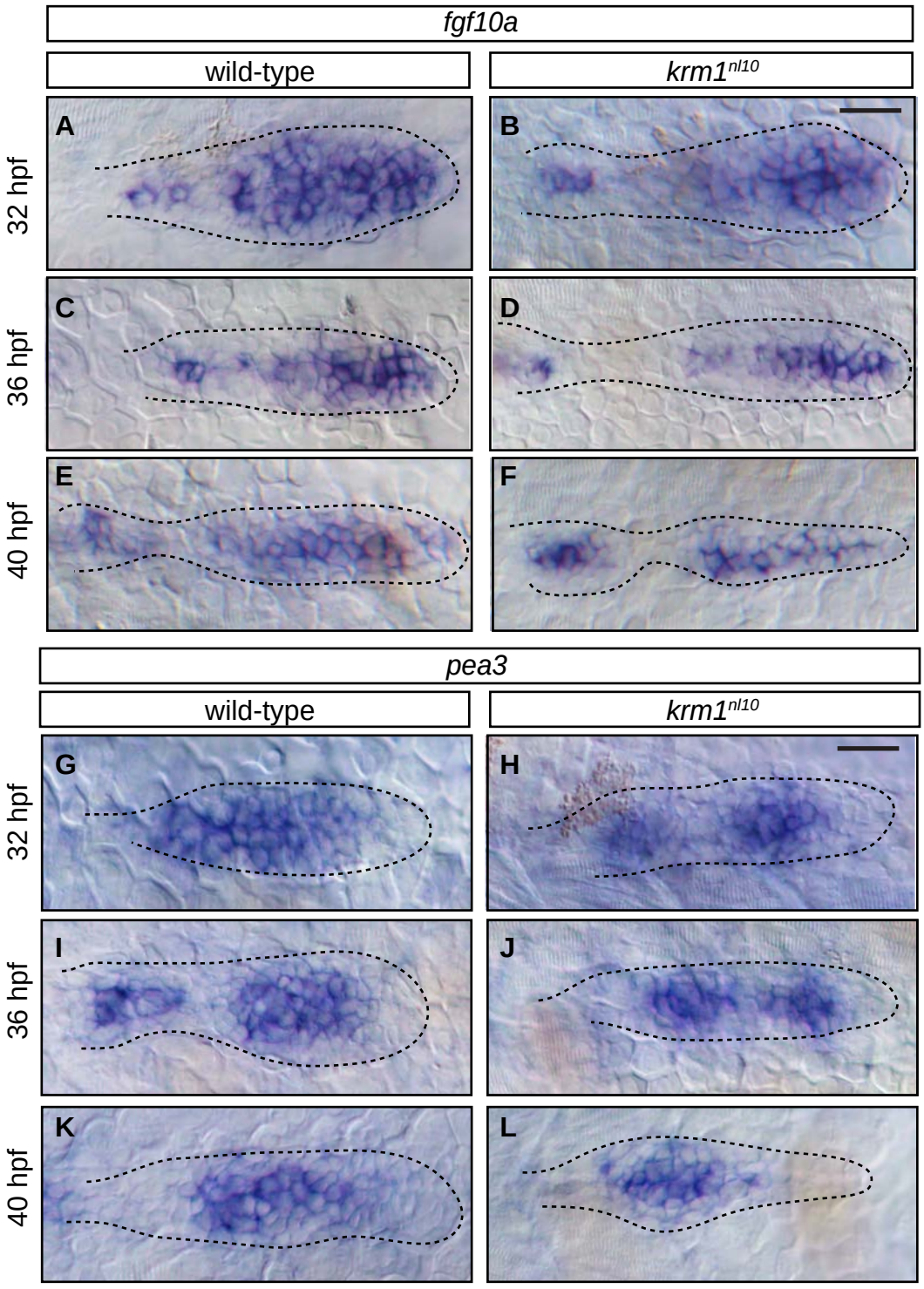
fgf10a
wild-type
krm1nl10
A
B
32 hpf
C
D
36 hpf
E
F
40 hpf
pea3
wild-type
krm1nl10
G
H
32 hpf
I
J
36 hpf
K
L
40 hpf

Figure S8

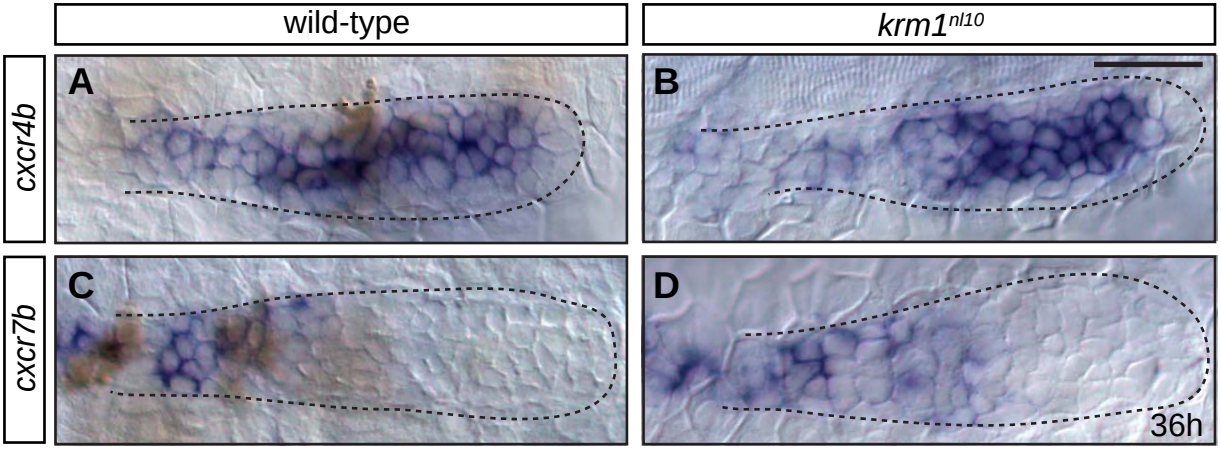

Figure S9

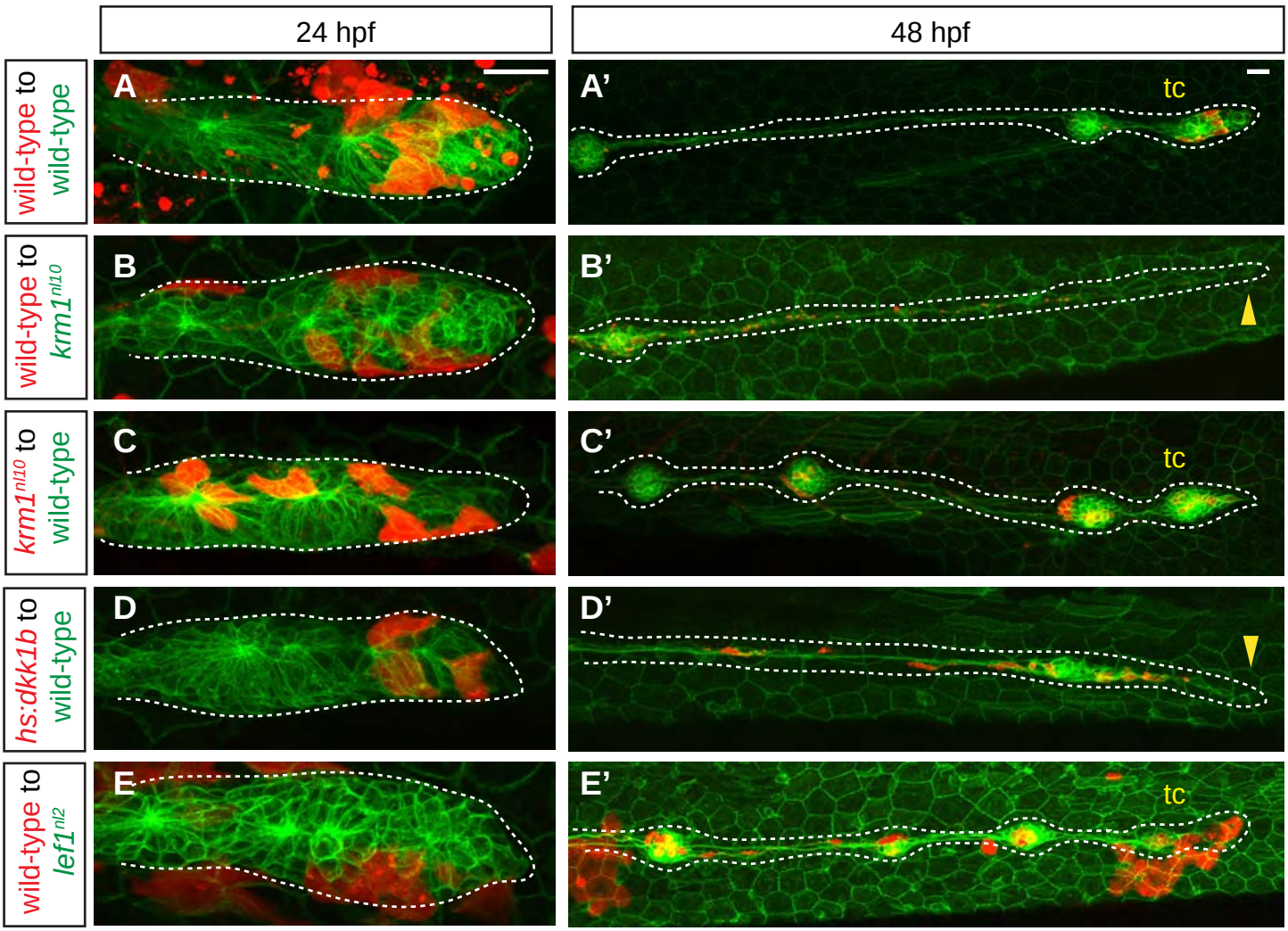
24 hpf
48 hpf
wild-type to wild-type
wild-type to krm1nl10
krm1nl10 to wild-type
hs:dkk1b to wild-type
wild-type to lef1nl2
A
A'
B
B'
C
C'
D
D'
E
E'
tc
tc
tc

Figure S10

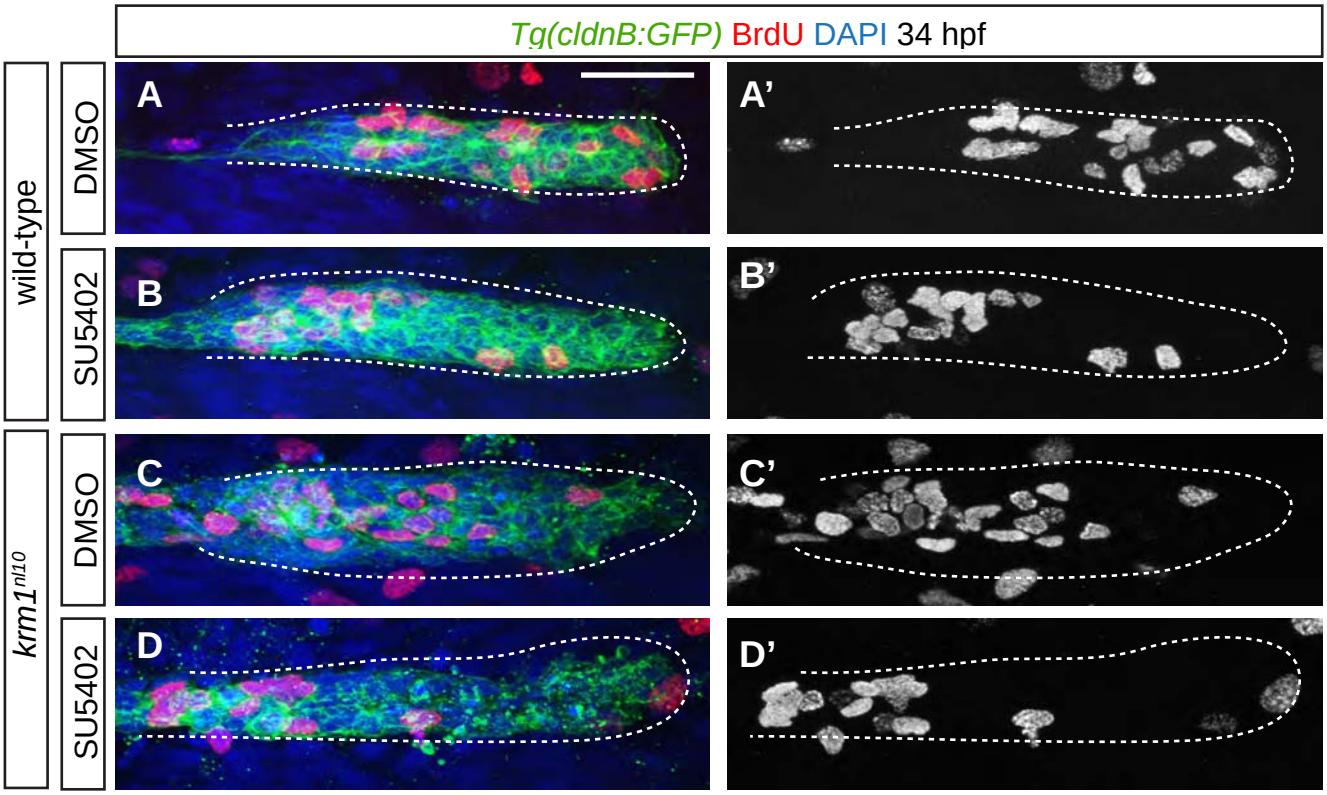
Tg(cldnB:GFP) BrdU DAPI 34 hpf
wild-type
krm1nl10
DMSO
SU5402
DMSO
SU5402
A
A'
B
B'
C
C'
D
D'

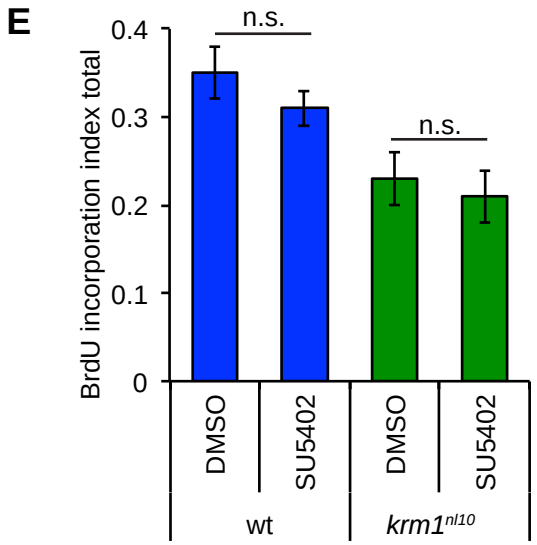
E
BrdU incorporation index total
0.4
0.3
0.2
0.1
0
n.s.
n.s.
DMSO
SU5402
DMSO
SU5402
wt
krm1nl10

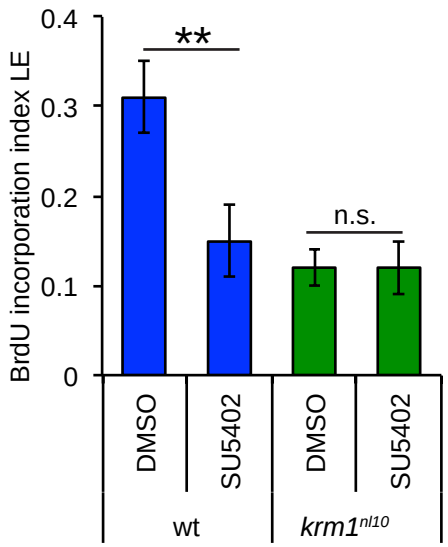
F
BrdU incorporation index LE
0.4
0.3
0.2
0.1
0
**
n.s.
DMSO
SU5402
DMSO
SU5402
wt
krm1nl10

Figure S11

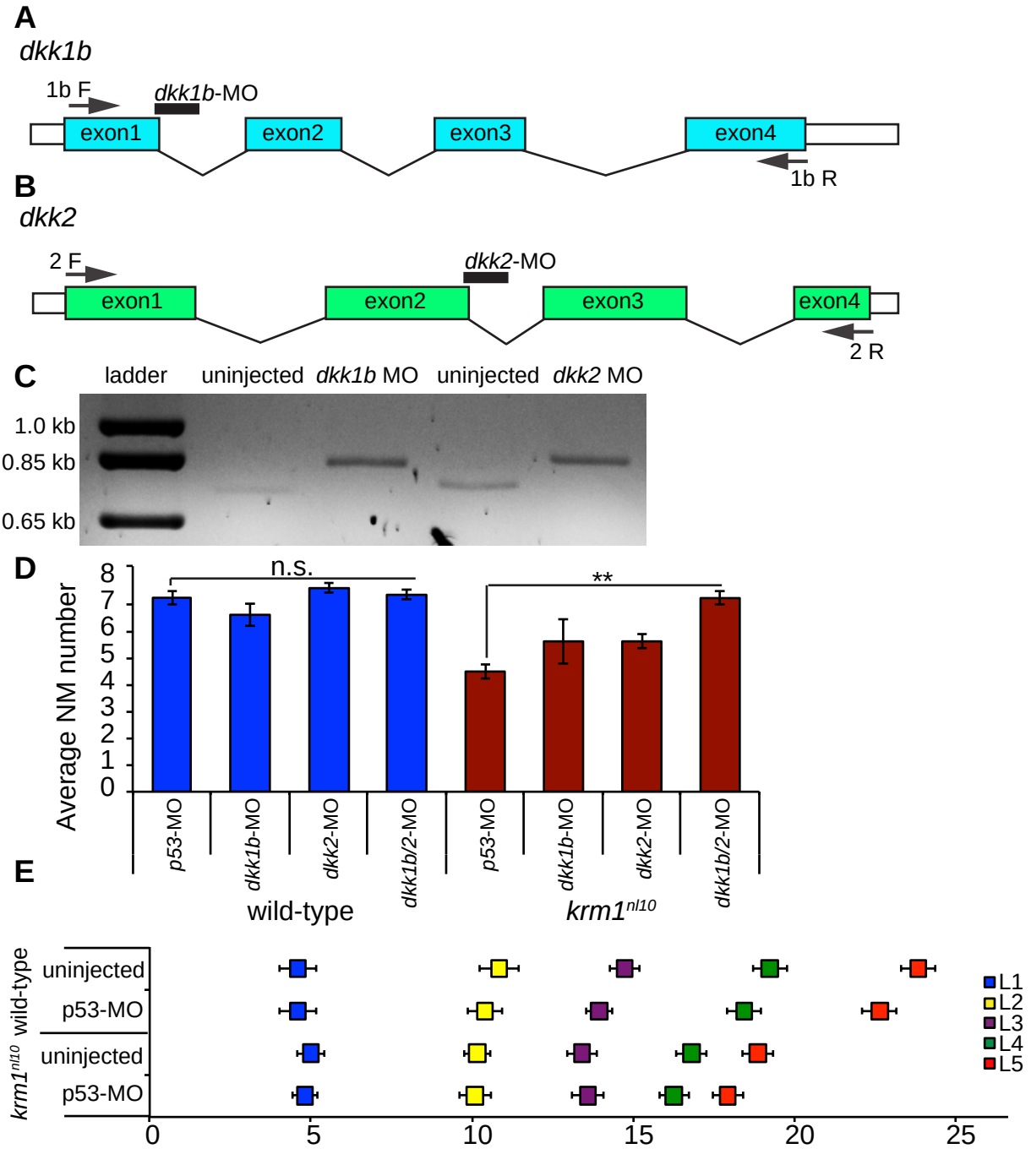
A
dkk1b
1b F
dkk1b-MO
exon1
exon2
exon3
exon4
1b R
B
dkk2
2 F
dkk2-MO
exon1
exon2
exon3
exon4
2 R
C
ladder
uninjected
dkk1b MO
uninjected
dkk2 MO
1.0 kb
0.85 kb
0.65 kb
D
Average NM number
n.s.
**
p53-MO
dkk1b-MO
dkk2-MO
dkk1b/2-MO
wild-type
krm1nl10
E
wild-type
krm1nl10
uninjected
p53-MO
uninjected
p53-MO
L1
L2
L3
L4
L5

Figure S12

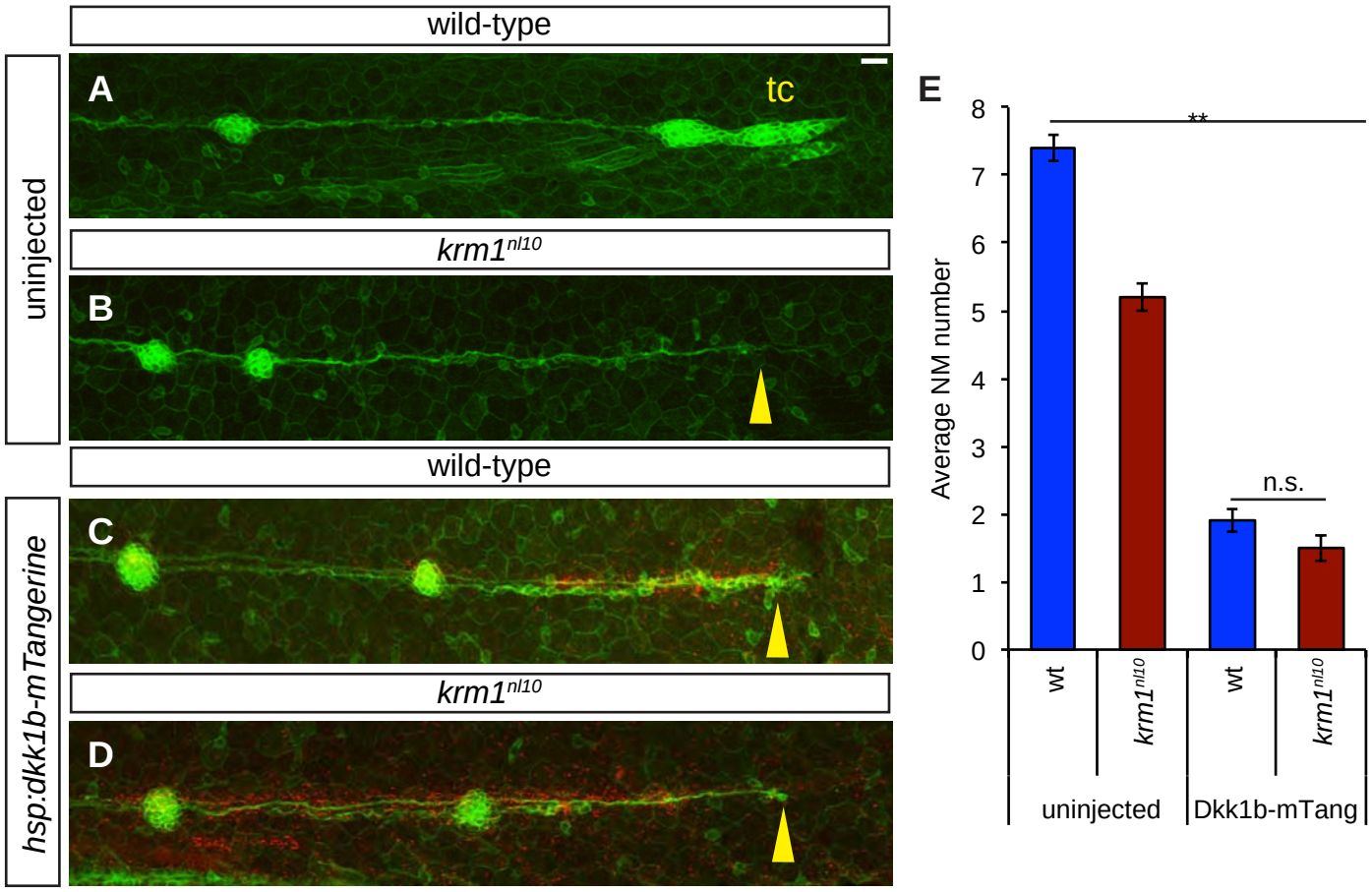

Tg(cldnB:GFP) Dkk1b-mTangerine 2 dpf

Figure S13

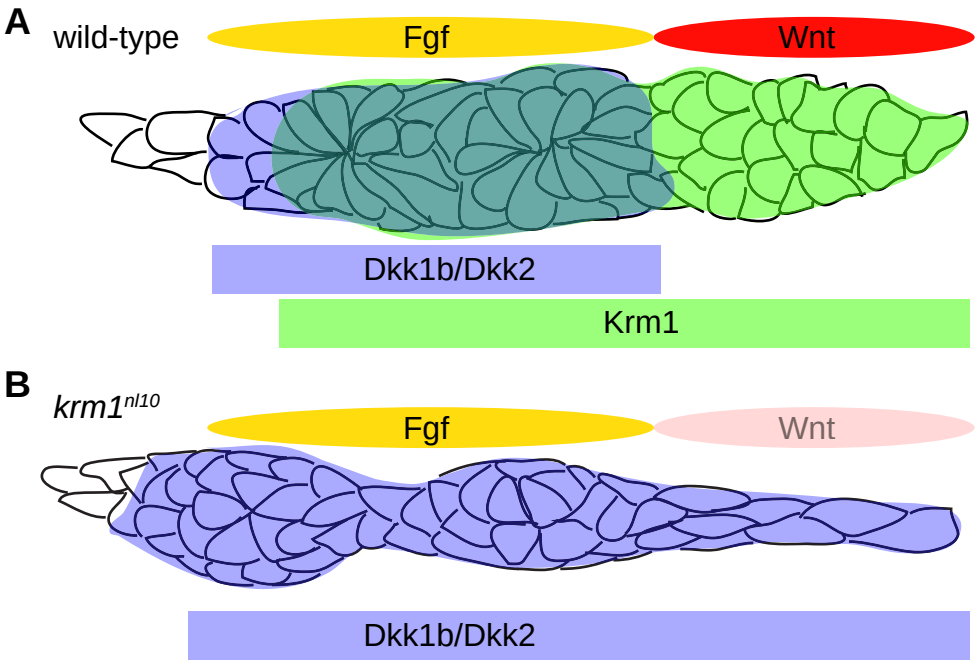
A
wild-type
Fgf
Wnt
Dkk1b/Dkk2
Krm1
B
krm1nl10
Fgf
Wnt
Dkk1b/Dkk2

Supplementary Movie Legends

Movie 1. Wild-type pLLP deposits NMs at regular intervals along the trunk
Time-lapse confocal projections of a *Tg(cldnB:GFP)*-positive wild-type pLLP imaged every 10 minutes for 15.5 hours starting at 36 hpf. During the course of imaging, the pLLP deposits 2 NMs and migrates out of the field to view. Scale bar: 100 μM.

Movie 2. pLLP migration fails in a *krm1*^{nl10} mutant
Time-lapse confocal projections of a *krm1*^{nl10} mutant pLLP labeled by *Tg(cldnB:GFP)* expression. Images were collected every 10 minutes for 15.5 hours beginning at 36 hpf. The mutant pLLP deposits 3 NMs before stalling and extending as a thin trail of cells. Scale bar: 100 μM.

Movie 3. Wnt sensor cells remain in the pLLP during migration
Live time-lapse confocal projections of a mosaic pLLP containing wild-type rhodamine labeled *Tg(7xtcf-siam:eGFP)*-positive and *Tg(7xtcf-siam:eGFP*)-negative donor cells in a wild-type *Tg(neuroD:eGFP)* host. Expression of *Tg(neuroD:eGFP)* marks extending pLL axons. Still images of this embryo at 24 and 48 hpf are shown in Fig. 5E,G. Images were collected every 10 minutes for 9.3 hours beginning at 34 hpf. During the course of migration, both GFP-positive and GFP-negative donors cells migrate along the trunk of the embryo. Scale bar: 100 μM.

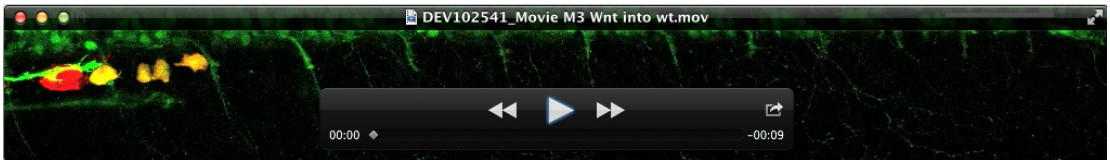

Movie 4. Wild-type donor cells fail to survive in a *krm1*^{nl10} mutant host
Live time-lapse confocal projections of a mosaic pLLP containing wild-type rhodamine labeled *Tg(7xtcf-siam:eGFP)*-positive and *Tg(7xtcf-siam:eGFP*)-negative donor cells in a *krm1*^{nl10} mutant *Tg(neuroD:eGFP)* host. Still images of this embryo at 24 and 48 hpf are shown in Fig. 5F,H. Images were collected every 10 minutes for 9.3 hours beginning at 34 hpf. Note that wild-type donor cells fragment and die (blue arrowhead) in the mutant pLLP during migration. Scale bar: 100 μM.